

Extending the low temperature operational limit of double-layer capacitors

Erik J. Brandon^{*}, William C. West, Marshall C. Smart, Larry D. Whitcanack, Gary A. Plett

Jet Propulsion Laboratory, California Institute of Technology, 4800 Oak Grove Drive, Pasadena, CA 91109, United States

Received 22 February 2007; received in revised form 29 March 2007; accepted 3 April 2007

Available online 7 April 2007

Abstract

This work describes the design and testing of organic electrolyte systems that extend the low temperature operational limit of double-layer capacitors (also known as supercapacitors) beyond that of typical commercially available components. Electrolytes were based on a tetraethylammonium tetrafluoroborate/acetonitrile system, modified with low melting co-solvents (such as formates, esters and cyclic ethers) to enable charging and discharging of test cells to as low as -75°C . Cell capacitance exhibited little dependence on the electrolyte salt concentration or the nature of the co-solvent used, however, both variables strongly influenced the cell equivalent series resistance (ESR). Minimizing the increase in ESR posed the greatest design challenge, which limited realistic operation of these test cells to -55°C (still improved relative to the typical rated limit of -40°C for commercially available non-aqueous cells).

© 2007 Elsevier B.V. All rights reserved.

Keywords: Supercapacitors; Electrochemical capacitors; Double-layer capacitors; Low temperature energy storage

1. Introduction

Batteries and fuel cells used for powering human and robotic spacecraft avionics are typically operated in a controlled thermal environment. In recent years, interest has grown in developing energy storage technologies and power delivery systems that can operate in the extreme temperatures of space with limited or no thermal control. This interest is motivated by the possibility of reducing the overall system mass of the avionics and simplifying the thermal management design, and has driven the successful development of low temperature lithium ion batteries in recent years [1]. Providing sufficient capacity and current levels at temperatures below -40°C continues to pose a challenge, however. High current pulses may reduce battery cycle life and require the battery to be sized accordingly, to meet peak current requirements. Due to the continuing need to minimize the mass and volume of avionics systems, it is worthwhile to consider new ways of storing and delivering charge at low temperatures, to complement existing battery technologies and minimize the power system mass.

Hybrid systems combining double-layer capacitors and batteries have been increasingly considered for use in terrestrial electronics applications, to maximize the energy and power density of the system [2]. These hybrid systems could play a similar role in space power applications. Double-layer capacitors, also known more colloquially as “supercapacitors,” have already been shown to be stable with respect to exposure to ionizing radiation [3]. Furthermore, due to the very nature of the charge storage mechanism, supercapacitors may be uniquely suited for storing energy at low temperatures.

Supercapacitor cells store charge within the double-layer formed between very high surface area electrodes and an electrolyte solution [2]. This charge storage mechanism leads to higher energy densities than are possible with conventional electrolytic capacitors, and higher power densities compared to electrochemical batteries. This combination of high energy and power densities arises from the very high capacitances that are possible, combined with the favorable charge/discharge kinetics associated with the double-layer.

Charging and discharging of batteries involve charge transfer and/or intercalation/deintercalation steps at the electrodes, in addition to transport of ions within the electrolyte. These Faradaic and mass transport processes are highly temperature dependent and thus more sluggish at low temperatures, limit-

^{*} Corresponding author. Tel.: +1 818 393 2674; fax: +1 818 393 5013.
E-mail address: erik.j.brandon@jpl.nasa.gov (E.J. Brandon).

ing the ability of the cell to deliver high currents. However, the charging and discharging steps in supercapacitors involve the rearrangement of the double-layer over very small distances, with no Faradaic or intercalation processes present at the electrode/electrolyte interface.

This set of conditions that exists for supercapacitors potentially provides a favorable situation for energy storage at low temperature, since the entropy contribution to the Gibbs electrostatic free energy should be reduced at low temperatures [2]. This reduction in entropy should in turn should lead to capacitance values which are similar or even slightly improved relative to room temperature values. In addition, other detrimental temperature dependent phenomena, such as current leakage, are minimized at these low temperatures (i.e., $<-40^{\circ}\text{C}$) [2].

Despite conditions which appear to favor very low temperature operation, -40°C represents the typical rated lower operational limit for non-aqueous based commercial off-the-shelf (COTS) cells [2]. COTS cells using aqueous based electrolytes and rated for operation to -50°C are available, however, they exhibit a lower energy density due to the more limited maximum operating voltage. Thus, in order for currently available supercapacitors to find use in space avionics, they will require special thermal control apart from the rest of the electronic subsystems, since most space-rated electronics are expected to operate to at least the -55°C limit. Supercapacitor cells have been characterized extensively down to the -40°C limit, mainly to study fundamental electrode processes and characterize leakage phenomena [4–6]. These data indicate cell performance is still acceptable at -40°C , leaving open the possibility for even lower temperature operation. There is a dearth of data for supercapacitors below this temperature limit, however, due to the relatively high freezing point of the solvents used in commercially available cells (propylene carbonate or acetonitrile). The most significant challenges in tailoring the electrolyte properties are to design electrolyte formulations with lower melting points while still maintaining adequate ionic conductivity, and to minimize the rise in equivalent series resistance (ESR) at lower temperatures caused by an increase in solvent viscosity.

The objectives of the study reported herein were to (1) tailor the electrolyte system to operate below -40°C , and (2) screen electrolytes to determine which systems result in a low ESR cell and (3) examine the DC charge/discharge characteristics of cells using these same systems. In addition to potentially leading to a practical device for low temperature operations in support of space exploration, these data may lend a greater understanding of fundamental cell processes (such as current leakage and the nature of the double-layer). Extension of the operating temperature to at least -55°C (the lower limit for most space rated electronics) would make these components more appealing for space applications.

Potential applications include augmenting high specific energy, low temperature primary battery cells or in designing hybrid supercapacitor-secondary battery cell systems to extend cell life in robotic space missions. Another potential application is for a “capacitor only” power supply for distributed sensor networks, where low temperatures are encountered and batteries are

difficult to replace (e.g., on planetary surfaces or in terrestrial Arctic monitoring stations). Finally, supercapacitors optimized for low temperature operation may find use in hybrid and electric vehicles, to improve performance during cold cranking and acceleration at low temperatures.

2. Experimental

2.1. Electrolyte preparation and cell assembly

Preparation of electrolyte solutions and cell assembly operations were conducted in an argon filled glovebox (Vacuum Atmospheres Company). Electrolyte solutions were prepared by dissolving tetraethylammonium tetrafluoroborate (TEATFB) at room temperature in the appropriate binary or ternary solvent system. Solvents used were acetonitrile (AN), ethyl acetate (EA), methyl formate (MF), methyl acetate (MA) and 1,3-dioxolane (DX). When 1,3-dioxolane was employed as the co-solvent, 2% by volume triethylamine (TEA) was added, to prevent acid catalyzed polymerization of the ether. Salt-free solvent blends were first prepared using a 3:1 volume ratio of acetonitrile to co-solvent (MA, EA, MF or DIOX) for use in melting point determination. Based on an initial evaluation of the melting points of these solvent blends and a consideration of the dielectric constant of the co-solvent, three of the solvent blends were chosen to formulate seven unique electrolyte systems, again using a 3:1 volume ratio of acetonitrile to co-solvent. The electrolyte systems ultimately chosen for study in test coin cells were 0.75 and 1 M TEATFB in 3:1 AN–MF, 0.25, 0.50, 0.75 and 1 M TEATFB in 3:1 AN–MA and 0.75 M TEATFB in 3:1 AN–DIOX. A 0.30 mm thick PACMM203 porous carbon material (Material Methods Corporation) was used for the electrodes. The thickness of the carbon electrode material was verified using a Conoscope Delta Z microscope and a micrometer. Hermetically sealed supercapacitor CR3032 coin cells (Hohsen Corporation) were used to evaluate the electrical properties of the electrode/electrolyte systems. Following metallization of the porous carbon material with ≥ 500 nm of RF sputtered platinum (to reduce contact resistance between the electrode and current collector casing), 1.6 cm diameter electrodes were punched and dried in a vacuum oven. The two carbon electrodes were electrically isolated from one another using a 20 μm thick polyethylene separator (Tonen-Setella). Cells were filled with the electrolyte solution, and an anode shim and wave spring placed in the cell to hold the electrode assembly firmly in place upon hermetic sealing. For electrochemical impedance spectroscopy (EIS), nickel contacts were spot welded onto the coin cell casing to minimize contacting issues with the test leads. Cells were also sealed with epoxy to prolong the hermetic seal of the cell.

2.2. Surface area and pore size distribution measurements

The methods of Brunauer, Emmett and Teller (BET), Barrett, Joyner and Halenda (BJH) and Horvath-Kawazoe were used to determine surface area and pore characteristics on a Micromeritics ASAP 2020 Gas Adsorption Analyzer [7]. Argon was used

as the adsorptive gas. Samples were degassed at 200 °C for 16 h prior to measurement.

2.3. Differential scanning calorimetry

Analysis of various mixtures was performed using a T.A. Instruments Model Q100 Differential Scanning Calorimeter (DSC) with refrigerated cooling system (RCS). Samples were encapsulated using aluminum hermetic DSC pans in an argon filled glove box and were weighed. Typical sample sizes were from 0.001 to 0.010 g. The DSC measurements were run using an argon purge at a flow of 50 mL min⁻¹. The samples were first cooled to -95 °C at a rate of 5 °C min⁻¹. As soon as the first run was completed, the sample was then run in the heating mode (also at 5 °C min⁻¹) back to 25 °C.

2.4. Conductivity measurements

Conductivity measurements of the electrolyte systems were made using two-electrode glass platinum cells (Orion Corporation). The cells were sealed (sealing operations were conducted inside of an argon glovebox) and then transferred to the thermal chamber where the conductivity was measured between the range of 25 and -65 °C.

2.5. Electrochemical impedance spectroscopy (EIS)

EIS measurements were performed using a Princeton Applied Physics VMP2 instrument. Data were collected over the frequency range of 100 kHz–10 mHz, at an excitation amplitude of 20 mV. Since the cells were measured in a temperature controlled chamber, direct connections to the cell with the four terminal instrument leads was not practical. The four instrument leads were connected to two wire leads attached with clamps to the nickel cell tabs. The ESR of the cell was taken as the real component of impedance where the imaginary component of impedance equals zero. Cells were held at temperature for 30 min before conducting the EIS measurements. At temperatures below -40 °C, multiple EIS measurements were conducted after longer soaks (at least 6 h) to assure that EIS measurement was stable against changes in the electrolytes, e.g., salt precipitation or phase separation. Data were taken upon cooling and upon heating, to determine if hysteretic effects were present.

2.6. DC capacitance measurements

To determine the DC capacitance and charging/discharging characteristics of cells using these electrolytes, coin cells were charged at a constant current of 1 or 25 mA to an open circuit voltage (V_{oc}) of 2.3 to 2.5 V. Cells were then discharged at the respective current, and the slope of the discharge curve determined from the linear region between 2 and 1 V. From this slope, the capacitance was extracted from $C = I/(dV/dt)$, where C is capacitance, I the discharge current and t is the time to discharge from 2 to 1 V. This cycle was then repeated at various temperatures between 25 and -80 °C, with data collected at periodic intervals.

3. Results and discussion

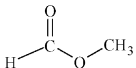
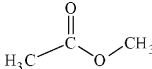
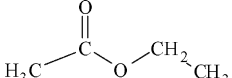
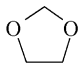
The overall goal of the present study was to evaluate several combinations of electrolyte/electrode systems designed to operate at temperatures below commercially available supercapacitor cells. As with supercapacitors optimized for room temperature operation, low temperature cells should exhibit both a suitable double-layer capacitance (to provide an adequate energy density) and low ESR (to achieve a high power density) across the desired operational temperature range. Double-layer capacitance at a given temperature is determined mainly by the accessible surface area of the electrode material, combined with the specific nature of the electrolyte system (e.g., aqueous versus non-aqueous). The cell ESR, however, is governed by the conductivity of the electrolyte solution and the electrode, separator and cell contact resistances.

The keys to meeting the above design objectives at low temperatures are to prevent freezing of the electrolyte, achieve sufficiently high electrolyte conductivity and maintain high salt concentration without precipitation. Optimizing these design parameters is made difficult by the fact that high conductivity solutions can best be achieved using an electrolyte with high salt concentrations. However, salt concentrations which are too high can lead to increased electrolyte viscosity at low temperature, leading to reduced ionic mobility, lower conductivity and higher ESR. Furthermore, salt solubility is typically compromised at lower temperatures, leading to the possibility of precipitation of salt in the pores of the electrode. In terms of specific solvent properties, therefore, a candidate electrolyte solvent should feature a melting point below the targeted operational temperature to prevent freezing, a high dielectric constant to minimize ion pairing and enhance salt solubility, a low viscosity to maximize ion mobility and a sufficiently wide electrochemical window at low temperatures.

Commercially available electrochemical capacitors may employ either aqueous or non-aqueous electrolytes [2,8,9]. Propylene carbonate or acetonitrile are typically used in non-aqueous based supercapacitors, in conjunction with a quaternary ammonium salt, such as TEATFB. Acetonitrile formulations combine a relatively high conductivity with a high room temperature salt solubility and a wide electrochemical window [2], and therefore represent a suitable starting point for low temperature electrolyte design.

With the typical commercial acetonitrile based systems, the freezing point extends to approximately -45 °C, leading to a typical low temperature rating of about -40 °C for most COTS supercapacitors. One method to achieve freezing point depression beyond this limit is through the formulation of binary solvent systems, in which appropriate low melting co-solvents are blended with the primary acetonitrile component. As stated earlier, the solvent system should be chosen to achieve the maximum freezing point depression while maintaining high salt solubility, low solution viscosity and favorable dielectric properties to the lowest achievable temperature limit. Based on their favorable electrochemical properties in low temperature battery work, organic formates, esters and cyclic ethers were considered as possible co-solvent candidates to form low temperature

Table 1
Physical properties for relevant solvents [11]

Solvent	Freezing point (°C)	Boiling point (°C)	Dielectric constant (ϵ)	Viscosity (cP)
$\text{H}_3\text{C}-\text{C}\equiv\text{N}$ Acetonitrile	-45.7	81.60	37.5	0.345 (25 °C)
 Methyl formate	-100	32	8.5	0.319 (29 °C)
 Methyl acetate	-98	56.9	6.68	0.38 (20 °C)
 Ethyl acetate	-83.6	77.1	6.0	0.426 (25 °C)
 1,3-Dioxolane	-95	78	7.3	0.6 (20 °C)

binary solvent systems [1]. The physical properties of some of these compounds are enumerated in Table 1.

The first step in developing and evaluating the low temperature electrolyte systems was to experimentally determine the freezing point of several candidate binary solvent systems. A 3:1 volume ratio of acetonitrile to co-solvent was chosen, to balance the need for an adequate depression of the freezing point with the need to maintain the favorable dielectric constant provided by acetonitrile. Several 3:1 blends of organic formates, esters or cyclic ethers with acetonitrile (no TEATFB salt) were prepared, and the freezing point determined by DSC (Table 2).

The next step in the process was to prepare and screen electrolyte solutions, selecting from solvent blends listed in Table 2 and varying the concentration of the added TEATFB salt. Commercially available cells typically employ TEATFB concentrations in the range of 0.1–1.5 M to maintain sufficient electrical conductivity and thus a high power density [10]. Similar concentrations were therefore chosen for the electrolytes in this study. Solution conductivity data were first collected to determine a range of expected electrolytic conductivity values versus temperature, relative to a benchmark solution of 1 M TEATFB dissolved in acetonitrile. The conductivity data for the electrolyte solutions display a range of room temperature values that are typical for non-aqueous electrolyte systems (Fig. 1).

Table 2
Freezing point data for 3:1 volume ratio acetonitrile/co-solvent mixtures (salt-free)

Co-solvent	Freezing point (°C)
Ethyl acetate	-72.0
Methyl formate	-71.0
Methyl acetate	-70.0
1,3-Dioxolane ^a	-67.9

Data are derived from differential scanning calorimetry, using the peak maximum temperature of the endotherm associated with the freezing phase transition (taken upon cooling).

^a Contains 2% by volume triethylamine stabilizer.

The expected drop in conductivity with a decrease in temperature is observed, due to the increase in solution viscosity and decrease in ionic mobility. The conductivity increased as concentration increased, converging to a narrower range of values at the lowest measured temperatures versus the initial room temperature conductivities. Of note is that all of the electrolyte systems screened for conductivity were still conductive below the point where acetonitrile is frozen (and displays no measurable electrolytic conductivity), and several displayed conductivities above 10 mS cm^{-1} at -60°C . With the exception of the 0.25 M TEATFB 3:1 AN–MA solution, varying amounts of precipitate were observed in the bottom of the conductivity cell after warming back to room temperature.

Next, two-electrode supercapacitor cells were prepared for screening of ESR versus temperature. A high surface area porous carbon material was used, with key surface area and pore parameters given in Table 3 and pore width versus the incremental surface area given in Fig. 2. The surface area value is typical of highly porous carbon materials employed in double-layer type supercapacitors.

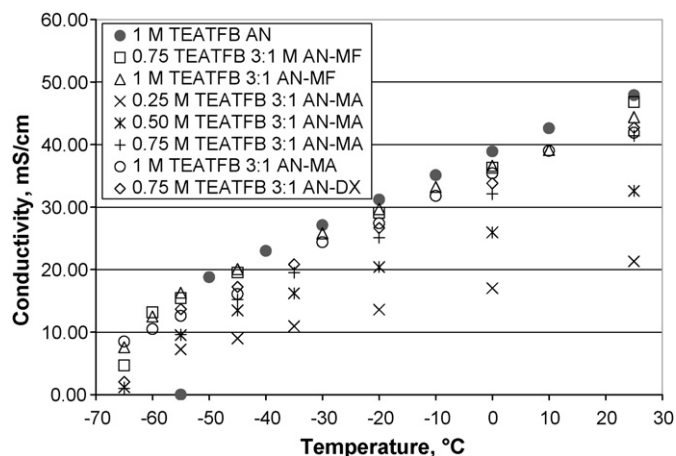


Fig. 1. Electrolyte conductivity vs. temperature for the reported electrolyte systems.

Table 3

Electrode surface area and pore characteristics for the porous carbon electrodes used in the test cells

BET surface area	1344 m ² g ⁻¹
BET adsorption average pore width	3.6 nm
BET desorption average pore width	3.6 nm
BJH adsorption average pore diameter	4.2 nm
Horvath-Kawazoe median pore width	0.93 nm

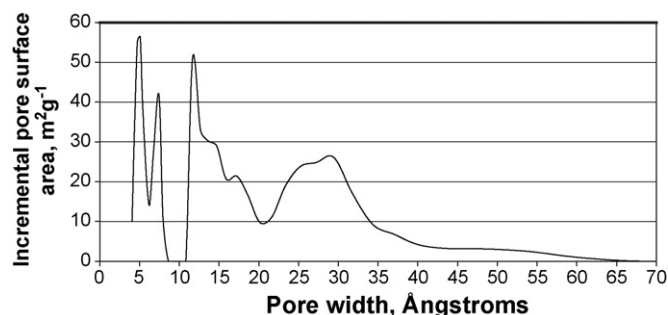


Fig. 2. Pore width vs. incremental pore surface area for the porous carbon electrodes.

The cell ESR values as measured via EIS included resistance associated with instrument leads, connections between the instrument and the cell, cell and nickel tabs, and so on. Typically, these ancillary resistance terms accounted for up to 0.35 Ω of the total ESR as measured using a coin cell with no separator or electrodes and the casing shorted. In most cases, the room temperature ESR was approximately 1 Ω, with the ESR steadily increasing down to -55 °C (Table 4). At -65 °C, the response of the cells no longer approximated that of a double-layer capacitor, with only an extremely high impedance signal present.

As indicated in Table 4, in the case of the 1 M TEATFB cells using the 3:1 AN-MA and 3:1 AN-MF solvent blends, there was either no measurable ESR value over the frequency range used (i.e., the real component of the impedance data did not intersect with the imaginary axis) or the response no longer approximated that of a stable, double-layer capacitor at the temperature indicated. This is likely indicative of a salt precipitation process within the electrode pores. Five cells did display measurable

Table 4

Equivalent series resistance as determined from the real component of the impedance where the imaginary component is zero

Formulation	ESR (Ω)				
	T = 25 °C	T = 0 °C	T = -20 °C	T = -45 °C	T = -55 °C
3:1 AN-MF					
0.75 M	0.722	0.798	0.919	1.20	1.42
1 M	0.621	0.709	0.817	46.6	^a
3:1 AN-MA					
0.25 M	1.04	1.20	1.40	1.87	2.21
0.50 M	0.955	1.12	1.41	1.60	1.86
0.75 M	0.717	0.820	0.954	4.74	7.04
1 M	1.43	1.78	^a	^a	^a
3:1 AN-DX ^a					
0.75 M	0.790	0.881	1.02	1.34	1.57

^a At these temperatures, the cells no longer exhibited a measurable ESR over the frequency range used or did not behave as a stable double-layer capacitor.

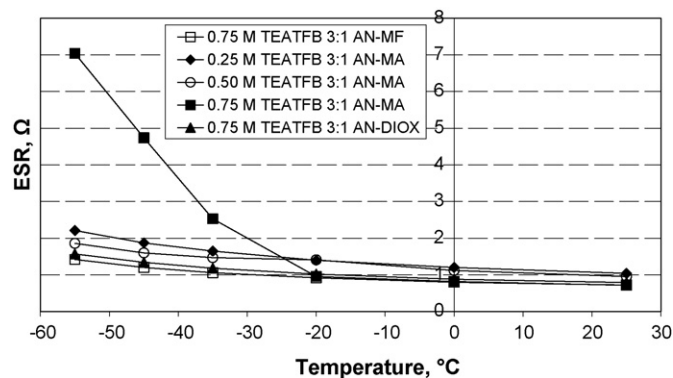


Fig. 3. Equivalent series resistance vs. temperature down to -55 °C, for five of the electrolyte blends.

values to the lowest temperatures to which data was collected, and the ESR data from Table 4 is plotted in Fig. 3. As seen, most of the cells display a similar response down to -55 °C, with the exception of the 0.75 M TEATFB 3:1 AN-MA cell. This is likely due to a slow precipitation of the salt with time, as discussed below.

Complex plane plots for the four cells with the lowest ESR are given in Figs. 4–7 (with data collected down to -65 °C). To about -55 °C, the observed behavior for 0.75 M TEATFB 3:1 AN-DX, 0.75 M TEATFB 3:1 AN-MF, 0.25 M TEATFB 3:1 AN-MA and 0.50 M TEATFB 3:1 AN-MA formulations is similar to that expected for a double-layer capacitor cell comprised of porous carbon electrodes down to -55 °C [2,9]. These four formulations form the basis of the most promising cells for operation down to -55 °C.

As seen in Fig. 8, for some solvent blends the impedance varied as a function of dwell time and electrolyte concentration, at low temperatures. This is clearly evident for the 3:1 AN-MA blend at 0.25 M (-55 °C), 0.75 M (-55 °C) and 1 M (-45 °C), where the impedance response changes significantly with dwell time as the electrolyte concentration is increased. The 1 M formulation displays very high impedance at -45 °C with no dwell (Fig. 8c). The 0.25 M formulation (Fig. 8a), however, leads to a stable impedance profile with time (after a 71 h dwell at -55 °C) whereas the 0.75 M formulation (Fig. 8b) exhibits an interme-

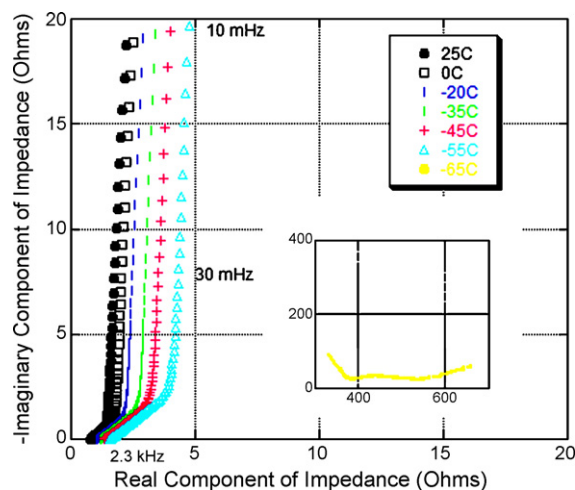


Fig. 4. 0.75 M TEATFB, 3:1 AN-DX electrochemical impedance complex plane plot. The -65°C data is given by the inset plot.

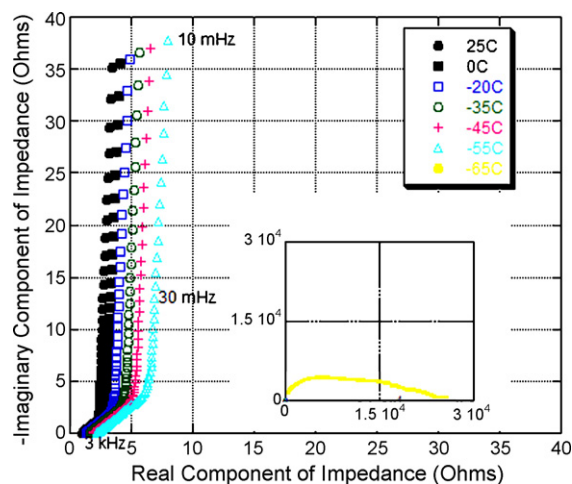


Fig. 7. 0.25 M TEATFB, 3:1 AN-MA electrochemical impedance complex plane plot. The -65°C data is given by the inset plot.

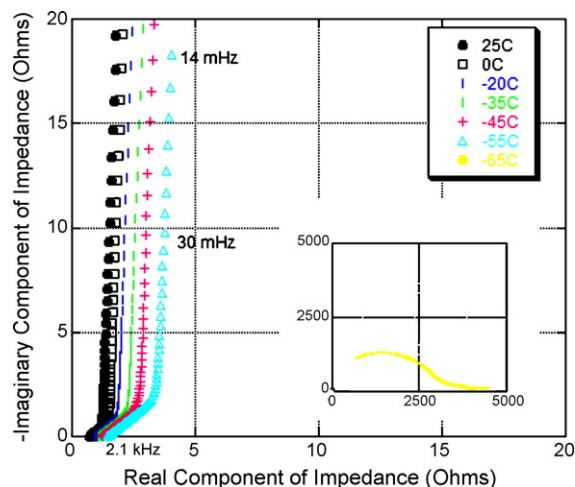


Fig. 5. 0.75 M TEATFB, 3:1 AN-MF electrochemical impedance complex plane plot. The -65°C data is given by the inset plot.

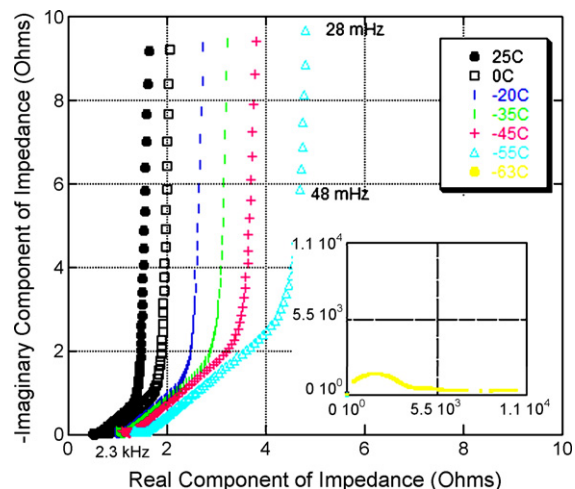


Fig. 6. 0.50 M TEATFB, 3:1 AN-MA electrochemical impedance complex plane plot. The -65°C data is given by the inset plot.

diate response under similar conditions. These observations are consistent with precipitation of salt at low temperatures, with the 0.25 M TEATFB 3:1 AN-MA electrolyte within the solubility limit at low temperature. As indicated, the 0.25 M TEATFB 3:1 AN-MA was the only one of all of the tested electrolytes that did not precipitate upon cooling to -65°C , with the 1 M TEATFB 3:1 AN-MA electrolyte yielding large platelet crystals under similar conditions.

The DC capacitance of the cells was then determined for each of the systems by constant current discharge measurements. The cells were charged at a current, I , of 1 mA to a working voltage, V_w , of 2.3 to 2.5 V. The capacitance was then determined from the slope of the 1 mA constant current discharge curve, along the linear region between 2 and 1 V. As seen in Table 5, despite the use of different solvent blends, the actual room temperature capacitance varied little. The mean cell capacitance and standard deviation taken at $+20^{\circ}\text{C}$ for the seven unique formulations reported here was $1 \pm 0.07 \text{ F cell}^{-1}$.

After determining the room temperature capacitance, the cells were taken through a series of charge/discharge cycles (at constant current, between 0.5 and 2.5 V) at various temperatures down to at least -65°C . If the cells were still operable at this temperature, additional data were collected down to -80°C . As indicated in Table 4, all of the cells could be discharged at temperatures below the typical commercially rated limit of -40°C , with near room temperature capacitance values maintained down to the -50 to -65°C range (depending on the specific formulation). The 0.75 M TEATFB 3:1 AN-DX blend could be charged and discharged as low as -75°C , maintaining about half of its room temperature capacitance.

In each case, cells were also cycled under a constant current charge/discharge regime at 25 mA, with the room temperature and lowest possible temperature data given in Table 5. The discharge curve for the three cells lowest ESR cells at -55°C are depicted in Fig. 9. At these higher currents, a very linear discharge is still maintained at -55°C . As seen in Table 5, many of the cells can still be readily discharged at -60°C with virtually no loss in capacitance versus the room temperature value.

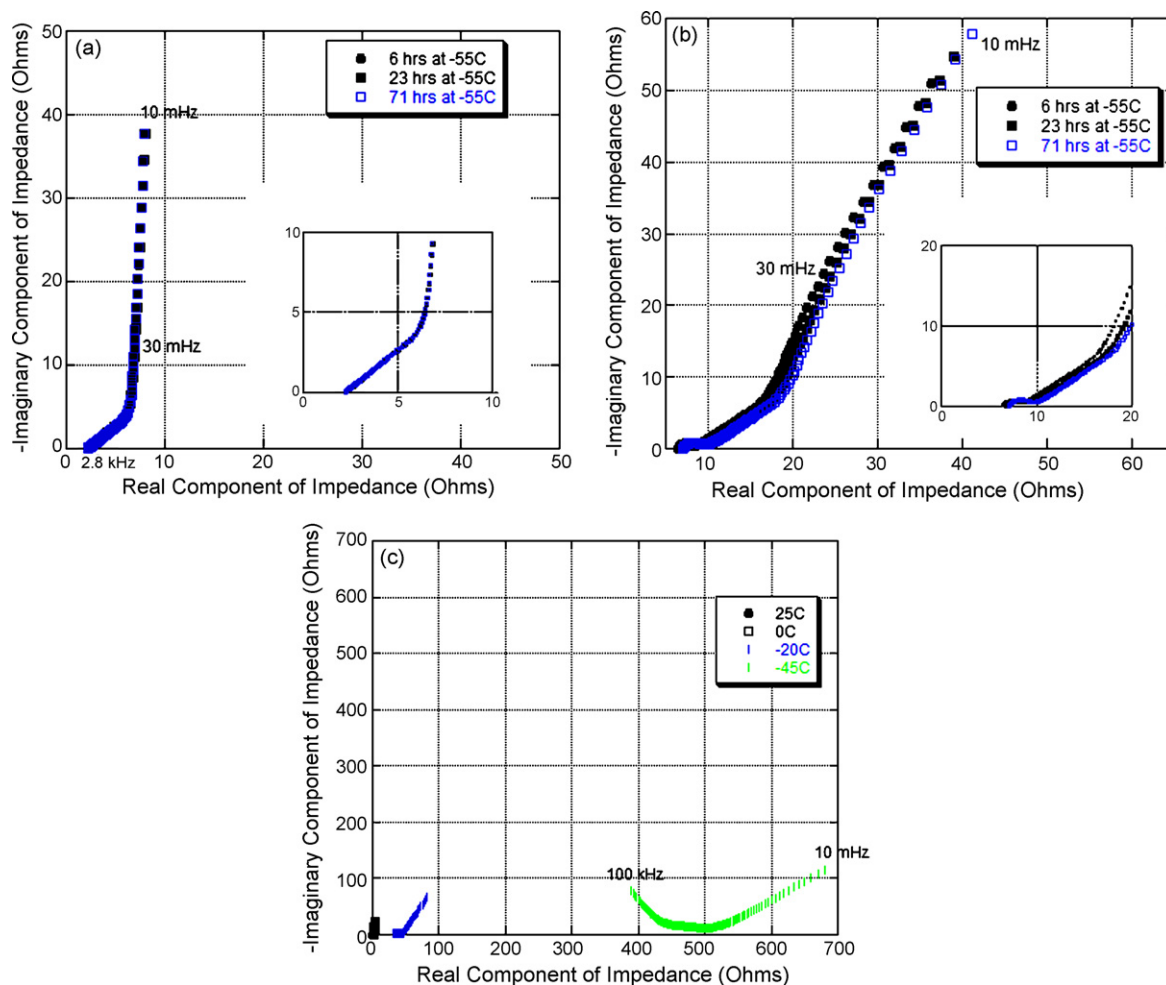


Fig. 8. Dependence of electrochemical impedance data on measurement dwell time and concentration of electrolyte. Data are all for a 3:1 AN–MA formulation at three different concentrations: 0.25 M at -55°C (a), 0.75 M at -55°C (b) and the 1 M at -45°C (c).

For this specific cell configuration, each single electrode was 1.6 cm in diameter, 0.30 mm thick, with a typical mass of ~ 0.0255 g for a total cell electrode volume and mass (sum of both electrodes) of 0.12 cm^3 per cell and 0.051 g per cell of active electrode material. Cells made with these three for-

mulations exhibited ESR values at -55°C between 1.45 and $1.86\ \Omega$, with a DC capacitance at 25 mA between 0.9 and 1.1 F at -60°C , leading to a specific gravimetric capacitance between 18 and $22\ \text{F g}^{-1}$ per cell. These values consider only the carbon electrode material, and will vary at the cell level in the final

Table 5
Capacitance data at 1 and 25 mA discharge currents

Formulation	20 °C Capacitance (F) (1 mA discharge)	Lowest T could charge at 1 mA (capacitance, F at T in parentheses)	20 °C Capacitance (F) (25 mA discharge)	Lowest T could charge at 25 mA (capacitance, F at T in parentheses)
3:1 AN–MF				
0.75 M	1.0	-50°C (1.0)	1.1	-60°C (1.1)
1 M	1.1	-60°C (1.0)	1.1	-55°C (1.1)
3:1 AN–MA				
0.25 M	0.9	-55°C (1.0)	1.1	-60°C (0.98)
0.50 M	1.0	-55°C (1.0)	1.0	-60°C (1.1)
0.75 M	1.0	-55°C (1.0)	1.0	-60°C (0.9)
1 M	1.0	-60°C (0.8)		Could not charge at 25 mA at 20 °C or below
3:1 AN–DX ^a				
0.75 M	0.9	-75°C (0.5)	1.0	-60°C (0.9)

^a Contains 2% by volume triethylamine stabilizer.

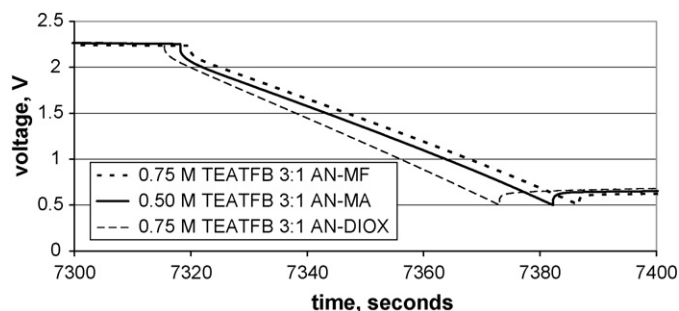


Fig. 9. Constant current discharge data at 25 mA and -55°C , for the three cells exhibiting the lowest ESR response at -55°C .

application depending on the degree of compression of the electrodes, and the mass of electrolyte, separator, current collector and packaging used. With stored energy given in Eq. (1) as:

$$E = \frac{1}{2} CV^2 \quad (1)$$

at a $V_w = 2.3\text{ V}$, the stored electrode specific energy is about $13\text{--}16\text{ Wh kg}^{-1}$ down to -60°C [2]. If the full mass of an actual cell is considered, this number will be reduced by well over half. This value would still be within the range of most commercially rated supercapacitors at room temperature (typically 5 Wh kg^{-1}). Power density is more difficult to determine and can be defined in numerous ways, since it depends on the state of charge of the capacitor and specific voltage range considered [2]. The maximum power density, P_{max} , can be determined by Eq. (2) [2]:

$$P_{\text{max}} = \frac{V^2}{4(\text{ESR})} \quad (2)$$

Since the cells were discharged through the internal resistance or ESR of the cell (which varied from 1.42 to $1.86\ \Omega$ at -55°C), if it is assumed that $V_w = 2.3\text{ V}$, the power density for these three optimal formulations is $\sim 15\text{ kW kg}^{-1}$ on a dry electrode basis at a temperature of -55°C , also assuming only the total mass of the carbon material in the cell.

4. Conclusions

Addition of appropriate co-solvents to the basic acetonitrile formulation can enable near room temperature double-layer capacitance at temperatures below -45°C , for the basic coin cell

configuration reported herein. In some cases, discharge down to -75°C is possible, with diminished capacitance. The key challenge to developing a suitable low temperature supercapacitor is maintaining a sufficiently low ESR. Acceptable ESR values could be maintained as low as -55°C with four of the formulations indicated previously. Further refinements in this capacitor system (such as tailoring the pore geometry and nature of the salt to optimize ion transport) may reduce this ESR even further. Efforts are continuing in this area to further improve the ESR at these and lower temperatures and thus increase the low temperature power density. Also under investigation are issues related to the lifetime of the cell (e.g., prolonged exposure at low temperature, leakage, etc.).

Acknowledgements

The authors would like to thank Steve Jaffe of Material Methods, Brian Wells of Auburn University and Tony Paris of the Jet Propulsion Laboratory (JPL) for helpful discussions; Mark Anderson of JPL for the electrode thickness measurements and the reviewers for helpful comments. This research was carried out at JPL, California Institute of Technology, funded through the JPL Research and Technology Development fund, under a contract with the National Aeronautics and Space Administration.

References

- [1] M.C. Smart, B.V. Ratnakumar, S. Surampudi, J. Power Sources 119–121 (2003) 906.
- [2] B.E. Conway, Electrochemical Supercapacitors: Scientific Fundamentals and Technological Applications, Kluwer-Plenum, New York, 1999.
- [3] S. Shojah-Ardalan, R. Wilkins, H.U. Machado, B.A. Syed, S. McClure, B. Rax, L. Scheick, M. Weideman, C. Yui, M. Reed, Z. Ahmed, IEEE Radiation Effects Data Workshop Conference Proceedings, Monterey, CA, July, 2003.
- [4] H. Gualous, D. Bouquain, A. Berthon, J.M. Kauffmann, J. Power Sources 123 (2003) 86.
- [5] R. Kotz, M. Hahn, R. Gallay, J. Power Sources 154 (2006) 550.
- [6] A. Janes, E. Lust, J. Electroanal. Chem. 588 (2006) 285.
- [7] A.W. Adamson, A.P. Gast, Physical Chemistry of Surfaces, Wiley-Interscience, New York, 1997.
- [8] M. Ue, K. Ida, S. Mori, J. Electrochem. Soc. 141 (1994) 2989.
- [9] M. Arulepp, L. Permann, J. Leis, A. Perkson, K. Rumma, A. Janes, E. Lust, J. Power Sources 133 (2004) 320.
- [10] Patent 5,621,607, Maxwell Technology.
- [11] Handbook of Chemistry and Physics, 87th ed., CRC Press, Cleveland, 2006.